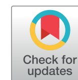

MmpL3 is the flippase for mycolic acids in mycobacteria

Zhujun Xu[a], Vladimir A. Meshcheryakov[a], Giovanna Poce[b], and Shu-Sin Chng[a,c,1]

[a]Department of Chemistry, National University of Singapore, Singapore 117543; [b]Dipartimento di Chimica e Tecnologie del Farmaco, Sapienza University of Rome, Rome 00185, Italy; and [c]Singapore Center on Environmental Life Sciences Engineering, National University of Singapore, Singapore 117456

Edited by Hiroshi Nikaido, University of California, Berkeley, CA, and approved June 5, 2017 (received for review January 3, 2017)

The defining feature of the mycobacterial outer membrane (OM) is the presence of mycolic acids (MAs), which, in part, render the bilayer extremely hydrophobic and impermeable to external insults, including many antibiotics. Although the biosynthetic pathway of MAs is well studied, the mechanism(s) by which these lipids are transported across the cell envelope is(are) much less known. Mycobacterial membrane protein Large 3 (MmpL3), an essential inner membrane (IM) protein, is implicated in MA transport, but its exact function has not been elucidated. It is believed to be the cellular target of several antimycobacterial compounds; however, evidence for direct inhibition of MmpL3 activity is also lacking. Here, we establish that MmpL3 is the MA flippase at the IM of mycobacteria and is the molecular target of BM212, a 1,5-diarylpyrrole compound. We develop assays that selectively access mycolates on the surface of *Mycobacterium smegmatis* spheroplasts, allowing us to monitor flipping of MAs across the IM. Using these assays, we establish the mechanism of action of BM212 as a potent MmpL3 inhibitor, and use it as a molecular probe to demonstrate the requirement for functional MmpL3 in the transport of MAs across the IM. Finally, we show that BM212 binds MmpL3 directly and inhibits its activity. Our work provides fundamental insights into OM biogenesis and MA transport in mycobacteria. Furthermore, our assays serve as an important platform for accelerating the validation of small molecules that target MmpL3, and their development as future antituberculosis drugs.

membrane biogenesis | lipid transport | trehalose monomycolate | Mycobacterial membrane protein Large | drug binding and inhibition

The outer membrane (OM) of *Mycobacterium tuberculosis*, the causative agent of tuberculosis (TB), is distinctively characterized by the abundance of mycolic acids (MAs), C_{60}–C_{90} long-chain, branched fatty acids packed together to produce a bilayer with markedly reduced fluidity and permeability (1). These MAs come in the forms of trehalose monomycolates (TMMs), trehalose dimycolates (TDMs), and mycolates covalently attached to arabinogalactan (AG) polysaccharides, which are, in turn, linked to the peptidoglycan and collectively known as the mAGP complex (Fig. 1*A*). MAs are synthesized at the inner membrane (IM) as TMMs via a highly conserved and well-characterized pathway (2), which is the target of the first-line anti-TB drug isoniazid (3). How MAs are transported across the cell envelope and assembled into the OM, however, is less well understood; proteins mediating TMM flipping across the IM and transit across the periplasm have not been identified and/or characterized (Fig. 1*A*). At the OM, the Ag85 complex transfers a mycolate chain from one TMM molecule to another to form TDM, or to the AG polysaccharides to form the mAGP complex (4). Tethering the OM to the cell wall via the AG polysaccharides further rigidifies the membrane, making it extremely impermeable to a wide range of compounds, including many antibiotics (1). The OM, and hence MAs, are essential for mycobacterial growth.

Recently, a conserved essential IM protein, Mycobacterial membrane protein Large 3 (MmpL3), has been implicated in MA transport. Depletion of MmpL3 in *Mycobacterium smegmatis* results in accumulation of TMMs and reduced formation of TDMs and AG-linked mycolates (5, 6), suggesting an impairment in TMM transport to the OM. Consistent with this finding, MmpL3, like other MmpL proteins, belongs to the resistance, nodulation, and cell division (RND) protein superfamily, and is believed to be a proton motive force (pmf)-dependent transporter (7). Based on its cellular localization, MmpL3 is likely involved in TMM flipping across the IM, TMM release from the IM into the periplasm, or both (Fig. 1*A*). However, its exact role has not been clearly defined, due largely to the lack of functional assays for its putative transport activity. Treatment of mycobacteria with a few structurally distinct small-molecule scaffolds, including ethylenediamines (e.g., SQ109) (8), 1,5-diarylpyrroles (e.g., BM212) (9, 10), adamantyl ureas (e.g., AU1235) (5), and others (11–15), results in similar changes in mycolate species as in MmpL3 depletion. These compounds inhibit growth and select for resistance mutations in *mmpL3*; however, there is limited evidence that they are direct MmpL3 inhibitors. The lack of activity assays for MmpL3 made it impossible to test the proposed mechanism of action of these putative inhibitors.

Here, we report that MmpL3 is the TMM flippase at the IM. Using a spheroplast model, we developed assays to monitor IM topology of TMM. We found that 1,5-diarylpyrrole BM212 inhibits TMM flipping across the IM in wild-type spheroplasts. Furthermore, we showed that specific MmpL3 variants confer resistance against this inhibition, indicating that MmpL3 is required for flipping TMM across the IM. Finally, we demonstrated that BM212 binds MmpL3 in vitro in a specific manner, and therefore directly targets MmpL3. Our work establishes lipid transport activity of a key member of the MmpL protein family, and highlights the importance of using small-molecule probes to interrogate protein function. Our assays have great utility in the

Significance

Biological membranes define cellular boundaries, allow compartmentalization, and represent a prerequisite for life; yet, our understanding of membrane biogenesis remains rudimentary. Mycobacteria, including the human pathogen *Mycobacterium tuberculosis*, are surrounded by a double-membrane cell envelope that makes them intrinsically resistant to many antibiotics. Specifically, the outer membrane (OM) contains unique lipids called mycolic acids (MAs), whose transport mechanism across the envelope is unknown. In this study, we established the role of an essential membrane protein as the flippase for MAs and demonstrated that this protein is a direct target of an antimycobacterial compound. Our work provides insights into OM biogenesis and lipid transport in mycobacteria, and the means to evaluate drugs that disrupt MA transport at the inner membrane.

Author contributions: Z.X. and S.-S.C. designed research; Z.X. performed research; Z.X., V.A.M., and G.P. contributed new reagents/analytic tools; Z.X. and S.-S.C. analyzed data; and Z.X. and S.-S.C. wrote the paper.

The authors declare no conflict of interest.

This article is a PNAS Direct Submission.

[1]To whom correspondence should be addressed. Email: chmchngs@nus.edu.sg.

This article contains supporting information online at www.pnas.org/lookup/suppl/doi:10.1073/pnas.1700062114/-/DCSupplemental.

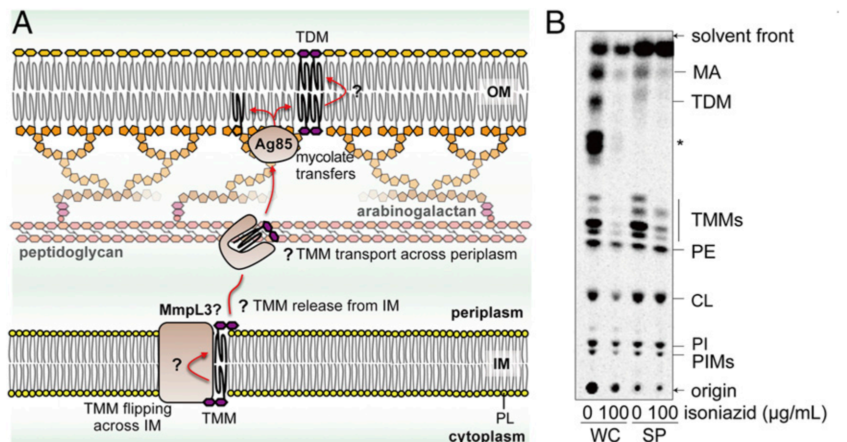

Fig. 1. TMM biosynthesis is intact in mycobacterial spheroplasts. (*A*) Schematic diagram illustrating the processes important for MA transport across the cell envelope. Following synthesis, TMMs must be flipped across the IM, released from the IM, and then transported across the periplasm (presumably via a chaperone). MmpL3 is implicated in TMM transport at the IM, but its exact role has not been elucidated. At the OM, the Ag85 complex transfers the mycolate chain from TMM to cell wall-linked AG polysaccharides or to another TMM to form TDM. Other known lipid species found in the OM and IM are omitted for simplicity. PL, phospholipid. (*B*) TLC analysis of newly synthesized [^{14}C]-labeled lipids extracted from wild-type *M. smegmatis* cells (WC) and spheroplasts (SP), visualized by phosphor imaging. Lipids were radiolabeled in the presence or absence of isoniazid as indicated. The developing solvent system comprises chloroform-methanol-water (30:8:1). A mycolate-based species that appears only in the presence of glucose is indicated with an asterisk. CL, cardiolipin; PE, phosphatidylethanolamine; PI, phosphatidylinositol; PIM, phosphatidylinositol mannoside.

validation and development of MmpL3-targeting small molecules as future anti-TB drugs.

Results

Spheroplasts Serve as a Viable System to Monitor TMM Topology. To develop a functional assay for TMM flipping across the IM, we sought a system where TMM topology in the IM can be monitored. Mycobacterial spheroplasts are ideal for this purpose because they are largely devoid of the OM and cell wall (16), and are bound only by the IM (17, 18), providing easy access to molecules of interest at this membrane. Due to the loss of periplasmic contents upon the formation of spheroplasts, we also expect the transport pathway(s) for TMM to the OM to be disrupted, thereby resulting in accumulation of TMM at the IM. *M. smegmatis* spheroplasts were successfully generated via sequential treatment with glycine and lysozyme (*SI Appendix*, Fig. S1), as previously reported (16). To examine whether MA synthesis is intact in spheroplasts, we profiled newly synthesized lipids metabolically labeled with [^{14}C]-acetate. Thin layer chromatography (TLC) analysis of lipids extracted from whole cells revealed a few major species whose syntheses are inhibited by isoniazid, indicating that these species are mycolate-based lipids (Fig. 1*B*). We assigned two of these species as TDM and TMM on the basis of reported retention factors of these lipids on TLC plates developed under the same solvent system (19). We showed that mycolates are still produced in *M. smegmatis* spheroplasts; however, the extracted lipids only contain TMM, and not TDM. Furthermore, we can no longer detect newly synthesized mAGP in the form of liberated mycolic acid methyl esters in these spheroplasts (*SI Appendix*, Fig. S2). These results are consistent with the loss of Ag85 enzymes and the OM, where TDM and mAGP syntheses occur, and also with the lack of TMM transport to any possible remnants of the OM. Given the extreme hydrophobicity of mycolates, we conclude that newly synthesized TMMs accumulate in the IM of spheroplasts, thus establishing a platform for monitoring TMM flipping across the bilayer.

TMMs Accumulated in Spheroplasts Reside in the Outer Leaflet of the IM. We next examined whether newly synthesized TMMs accumulated in the inner or outer leaflet of the IM in spheroplasts by monitoring its accessibility to degradation by recombinant LysB, a lipolytic enzyme. LysB is a mycobacteriophage-encoded esterase that is specific for mycolates and plays the role of an endolysin important for the release of phage particles from infected cells (20, 21). Substantial amounts (~77%) of newly synthesized TMMs in spheroplasts are readily and specifically hydrolyzed by purified LysB with the concomitant release of MAs (Fig. 2*A*). Part of this hydrolysis can be attributed to the background exposure of TMMs to LysB in a subset of spheroplasts that lysed during the experiment (~30–50% cell lysis irrespective of the addition of LysB; Fig. 2*B* and *SI Appendix*, Fig. S3). The remaining newly synthesized TMMs that were cut by LysB are likely accessible on the surfaces of intact spheroplasts. We showed that an inactive LysB variant does not result in the same effect (Fig. 2*A*). In addition, we demonstrated that LysB does not enter intact spheroplasts (Fig. 2*B*), and that it does not induce additional cell lysis compared with controls (Fig. 2*B* and *SI Appendix*, Fig. S3). Taken

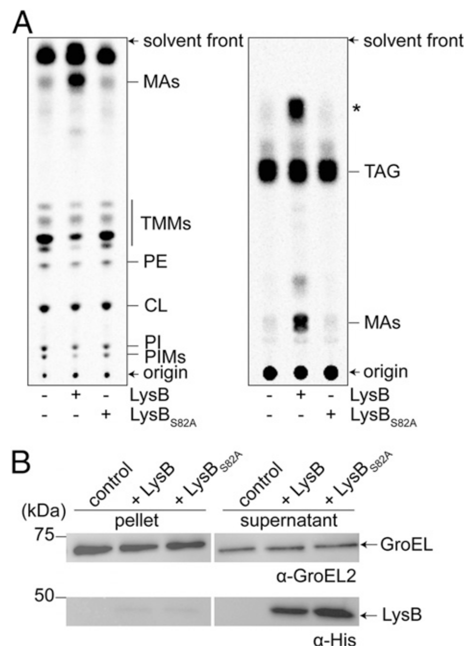

Fig. 2. Newly synthesized TMMs in mycobacterial spheroplasts are accessible to degradation by LysB, indicating that these TMMs reside in the outer leaflet of the IM. (*A*) TLC analyses of newly synthesized [^{14}C]-labeled lipids extracted from *M. smegmatis* spheroplasts treated with functional or nonfunctional (S82A) LysB. Lipids were resolved on TLCs developed using solvent systems comprising either chloroform-methanol-water (30:8:1) (*Left*) or hexane-diethylether-acetic acid (70:30:1) (*Right*), followed by phosphor imaging. In addition to MA, treatment with functional LysB resulted in the release of an unidentified apolar lipid, annotated with an asterisk. TAG, triacylglycerol. (*B*) α-GroEL2 and α-His immunoblot analyses of pellet and supernatant fractions obtained from sedimentation of *M. smegmatis* spheroplasts treated with functional or nonfunctional (S82A) LysB.

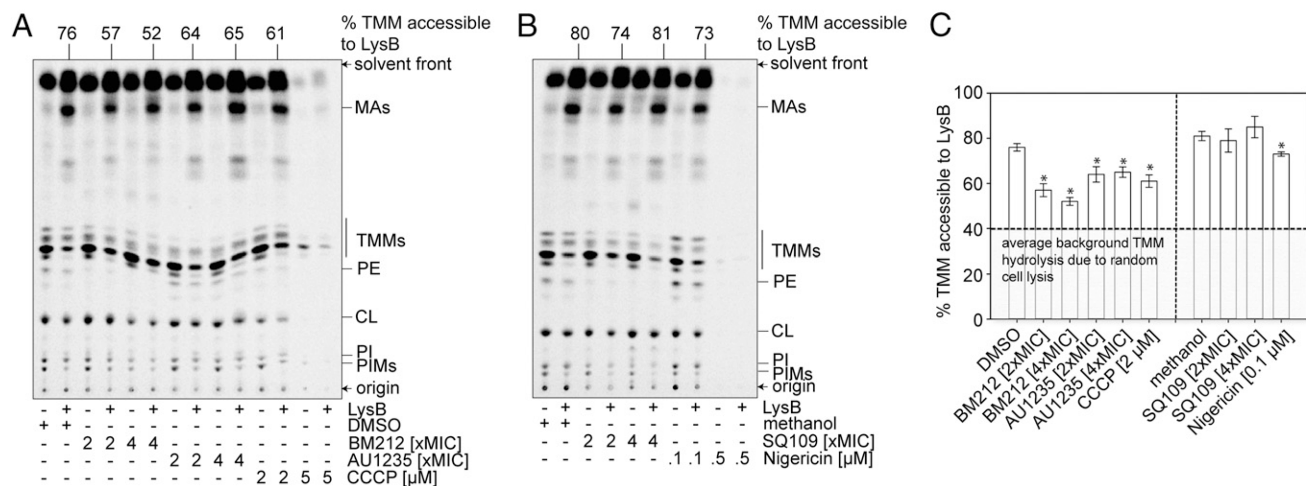

Fig. 3. Antimycobacterial compounds BM212 and AU1235 reduce TMM accessibility to LysB in spheroplasts, indicating inhibition of TMM flipping across the IM. Representative TLC analyses of [^{14}C]-labeled lipids newly synthesized in the presence of indicated concentrations of BM212 and AU1235 (*A*) and SQ109 (*B*), and extracted from *M. smegmatis* spheroplasts following treatment with or without purified LysB. The effects of pmf disruptors, carbonyl cyanide *m*-chlorophenyl hydrazone (CCCP) and nigericin were also tested. At higher concentrations, these uncouplers affected lipid synthesis, consistent with the depletion of ATP. DMSO and methanol were used to dissolve the respective compounds, and thus serve as negative controls. Equal amounts of radioactivity were spotted for each sample. The developing solvent system comprises chloroform-methanol-water (30:8:1). (*C*) Graphical plot showing the effects of various compounds on the amounts of LysB-accessible TMMs in spheroplasts. The percentage of TMMs accessible to LysB is given by the difference in TMM levels between samples with or without LysB treatment, normalized against the level in control samples without LysB treatment. TMM levels in each sample were quantified as a fraction of total mycolates (TMM + MA). Average percentages and SDs from three biological replicates are plotted. The average background of TMM hydrolysis due to random cell lysis during the experiment (~40%) is indicated. Student's *t* test: *$P < 0.05$ compared with the corresponding DMSO or methanol controls.

together, these results establish that most newly synthesized TMMs have been translocated across the IM in intact spheroplasts, and therefore reside in the outer leaflet of the membrane.

MmpL3 Is Responsible for Flipping TMM Across the IM. Several compounds, including SQ109, BM212, and AU1235, are believed to affect MmpL3-mediated TMM transport because mutations in *mmpL3* confer resistance against these small molecules

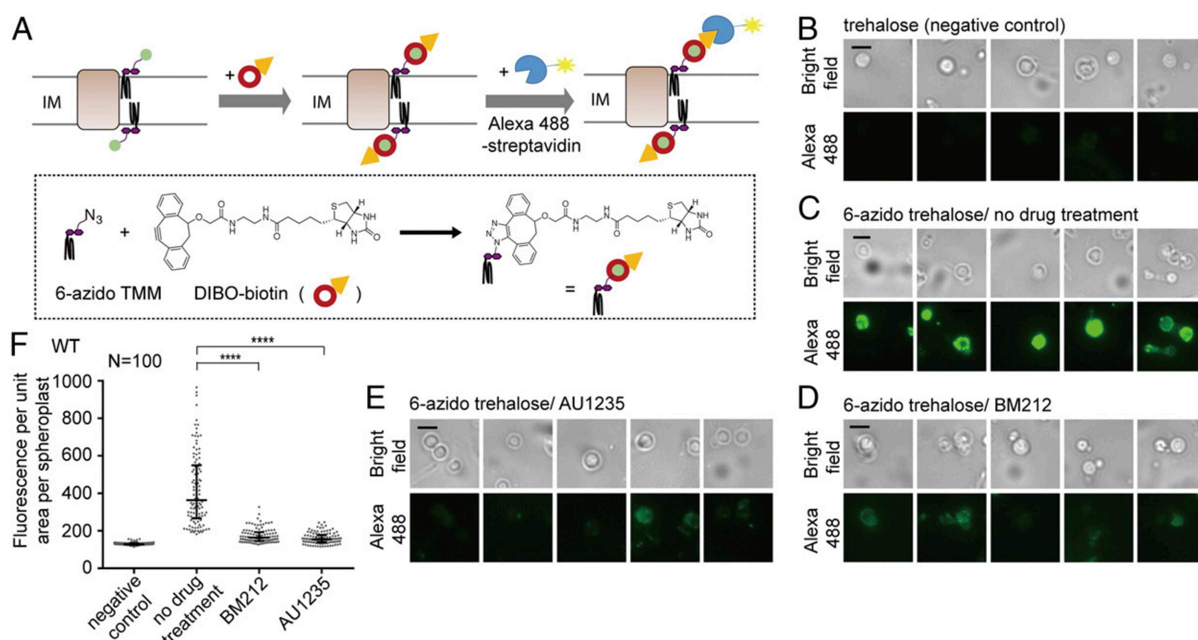

Fig. 4. Antimycobacterial compounds BM212 and AU1235 reduce surface display of 6-azido-TMMs in spheroplasts, indicating inhibition of TMM flipping across the IM. (*A*) Schematic diagram illustrating the 6-azido-TMM surface display assay. Spheroplasts were incubated with 6-azido-trehalose to allow synthesis of 6-azido-TMMs (22), which were subsequently labeled with alkyne-containing biotin (DIBO-biotin) via click chemistry (23). Surface-exposed biotin-TMMs were recognized by Alexa Fluor 488-conjugated streptavidin and visualized by fluorescence microscopy. Representative bright-field and fluorescence microscopy images are shown following DIBO-biotin/Alexa Fluor 488-streptavidin labeling of spheroplasts synthesizing TMM (*B*), or 6-azido-TMM in the presence of DMSO (*C*), BM212 (*D*, twofold MIC), and AU1235 (*E*, twofold MIC). (Scale bars: 3 μm.) (*F*) Fluorescence intensity per unit area for individual spheroplasts ($n = 100$) in each condition in *B*–*E* is plotted, with the medians and interquartile ranges indicated. Mann–Whitney test: ****$P < 0.0001$ compared with the "no drug treatment" control.

Fig. 5. Mutations in MmpL3 render BM212 less effective in the inhibition of TMM flipping across the IM. Representative TLC analyses of [^{14}C]-labeled lipids newly synthesized in the presence of indicated concentrations of BM212 and extracted from wild-type (WT) (*A*), $mmpL3_{V197M}$ (*B*), and $mmpL3_{A326T}$ (*C*) *M. smegmatis* spheroplasts following treatment with or without purified LysB are shown. Equal amounts of radioactivity were spotted for each sample. The developing solvent system comprises chloroform-methanol-water (30:8:1). (*D*) Graphical plot showing the dose-dependent effects of BM212 on the percentage of TMMs accessible to LysB in the respective spheroplasts (quantification as per Fig. 3). Average percentages and SDs from three biological replicates are plotted. The average background of TMM hydrolysis due to random cell lysis during the experiment (~40%) is indicated. Student's *t* test: $^{*}P < 0.05$, $^{**}P < 0.01$ compared with the corresponding DMSO controls for each respective strain. Representative bright-field and fluorescence microscopy images are shown following DIBO-biotin/Alexa Fluor 488-streptavidin labeling of $mmpL3_{V197M}$ spheroplasts synthesizing TMM (*E*), 6-azido-TMM in the presence of DMSO (*F*) and 6-azido-TMM in the presence of BM212 (*G*, twofold MIC). (Scale bars: 3 μm.) (*H*) Fluorescence intensity per unit area for individual spheroplasts (n = 100) in each condition in *E*–*G* is plotted, with the medians and interquartile ranges indicated. Mann–Whitney test: N.S., not significant ($P > 0.5$ compared with the "no treatment" control).

(5, 8, 9). Although it is not yet clear if these compounds directly inhibit MmpL3, they may be useful as probes to determine if MmpL3 is responsible for TMM flipping across the IM. Specifically, we asked whether these small molecules are able to inhibit TMM flipping in wild-type spheroplasts, and whether they would become less effective in doing so in spheroplasts expressing MmpL3 variants that confer resistance against them. We first tested the effects of these compounds in our LysB assay in wild-type spheroplasts. Remarkably, BM212 and AU1235 are able to reduce LysB-mediated hydrolysis of newly synthesized TMMs in *M. smegmatis* spheroplasts (Fig. 3 *A* and *C*), at concentrations twofold and fourfold above their reported minimal inhibitory concentrations (MICs) (5, 9) (*SI Appendix*, Table S1). In contrast, SQ109 has no effect (Fig. 3 *B* and *C*). For BM212, hydrolysis by LysB is strongly reduced, close to the level of background attributed to nonspecific spheroplast lysis (*SI Appendix*, Fig. S3). We showed that the effects of BM212 and AU1235 are not due to direct inhibition of LysB activity, because TMMs are still hydrolyzed in detergent-solubilized samples (*SI Appendix*, Fig. S4). Instead, significant amounts of newly synthesized TMMs are no longer accessible to LysB in the presence of either compound in intact spheroplasts, indicating inhibition of TMM flipping across the IM. As an alternative method to assess TMM topology in the IM and the effects of these drugs, we also examined the ability of membrane-impermeable fluorophore-conjugated streptavidin to bind to newly synthesized TMMs engineered to contain biotin (biotin-TMMs) (Fig. 4*A*). Here, we metabolically labeled TMMs with 6-azido-trehalose (22), which allowed us to attach an alkyne-containing biotin probe covalently to TMM via the bioorthogonal click reaction (23). In wild-type spheroplasts, biotin-TMMs can be detected on the surface, indicating that 6-azido-TMMs have been translocated across the IM (Fig. 4 *C* and *F*). Biotin labeling of 6-azido-trehalose groups, and therefore detection with streptavidin, was largely prevented if LysB was added (*SI Appendix*, Fig. S5), confirming that we are visualizing trehalose-linked mycolates (i.e., TMMs) at the IM in spheroplasts. We demonstrated that both BM212 and AU1235 drastically reduce the amounts of 6-azido-TMMs, and hence biotin-TMMs, that can be labeled with streptavidin (Fig. 4 *D*–*F*). Again, SQ109 is not effective in this assay (*SI Appendix*, Fig. S6). Consistent with the LysB accessibility assay, these results establish that BM212 and AU1235, but not SQ109, inhibit TMM flipping across the IM.

To establish whether MmpL3 is responsible for flipping TMM across the IM, we used specific MmpL3 variants that render *M. smegmatis* cells less sensitive to BM212, and tested if TMM flipping in spheroplasts expressing these variants would be more

Fig. 6. BM212 binds MmpL3 in vitro in a specific manner. (*A*) Representative Clear Native-PAGE analyses of purified MmpL3-His samples incubated with increasing concentrations of [^{14}C]-BM212, visualized separately by phosphor imaging and Coomassie blue (CB) staining. The amount of [^{14}C]-BM212 bound to MmpL3 at each concentration was quantified, normalized to the amount at maximum binding, averaged across triplicates, and plotted. Error bars represent SDs. The data were fitted to a "one-site–specific binding" model using nonlinear regression (K_d = 65.5 ± 17.9 μM). (*B*) Clear Native-PAGE analyses of purified MmpL3-His samples incubated with a fixed concentration of [^{14}C]-BM212, but in the presence of increasing concentrations of cold BM212. Gels were visualized separately by phosphor imaging and CB staining. (*C*) Mutations that confer resistance against BM212 cluster on a structural model of MmpL3, suggesting a possible binding site. A Phyre2 (35) structural model for *M. smegmatis* MmpL3 without its C-terminal cytoplasmic domain is shown in side (*Left*) and top (*Right*) views. For clarity, periplasmic domains are removed from the top-view image. Residues important for passage of protons are highlighted in black. Residues that conferred resistance against BM212 (10) when mutated in MmpL3 from *M. smegmatis*, *Mycobacterium bovis bacillus Calmette–Guérin*, and *M. tuberculosis* are highlighted in red, purple and cyan, respectively.

resistant to the effects of BM212. The growth of cells expressing $MmpL3_{V197M}$ or $MmpL3_{A326T}$ variants is only fully inhibited in the presence of four- to eightfold the concentration of BM212 that inhibits wild-type growth (9) (*SI Appendix*, Table S1). We showed that BM212 does not affect MmpL3 levels in wild-type spheroplasts (*SI Appendix*, Fig. S7); yet, it strongly inhibits TMM flipping in a dose-dependent manner (Fig. 5 *A* and *D*). We further demonstrated that BM212 is less effective at reducing LysB accessibility to TMM in spheroplasts expressing $MmpL3_{V197M}$ or $MmpL3_{A326T}$ variants (Fig. 5 *B–D*). In fact, BM212 is also unable to inhibit the display of 6-azido-TMMs on the surface of spheroplasts expressing $MmpL3_{V197M}$ (Fig. 5 *E–H*). Because TMM is only accessible on the outer leaflet of the IM in the presence of functional MmpL3 (i.e., not inhibited by BM212), we conclude that MmpL3 is the TMM flippase.

BM212 Binds and Directly Inhibits MmpL3 Function. MmpL3 function is believed to require the pmf, specifically the proton gradient (7). Consistently, we showed that proton gradient uncouplers, such as carbonyl cyanide *m*-chlorophenyl hydrazone and nigericin (Fig. 3), but not membrane potential disruptors, such as valinomycin-K^+ (*SI Appendix*, Fig. S8), can inhibit LysB accessibility to TMMs in spheroplasts. Whether BM212 inhibits TMM flipping by directly targeting MmpL3 is not clear. Contrary to previous reports (24), we did not observe effects on the proton gradient (*SI Appendix*, Table S2) or the membrane potential (*SI Appendix*, Fig. S10) in spheroplasts treated with BM212 at concentrations that inhibited TMM flipping. Therefore, BM212 does not inhibit MmpL3 via indirect effects on the pmf. To determine if BM212 directly targets MmpL3, we examined the ability of BM212 to bind physically to purified MmpL3 (*SI Appendix*, Fig. S11) in vitro. We demonstrated that [^{14}C]-BM212 binds purified wild-type MmpL3 in a saturable manner, with an apparent K_d of ~66 μM (or ~27 μg/mL) (Fig. 6*A*). Given that the binding assay was performed using purified MmpL3 solubilized in detergent (as opposed to being in a native lipid bilayer), it is highly likely that this K_d value is overestimated; the real K_d of [^{14}C]-BM212 binding to MmpL3 may thus be closer to the MIC (~7.6 μM or 3.1 μg/mL), consistent with a specific binding event. To corroborate this finding, we further showed that this interaction can be competed away by excess nonlabeled BM212 (~100-fold above saturation binding) (Fig. 6*B*), indicating that BM212 can bind to MmpL3 in a specific manner. In fact, mutations in *mmpL3* that confer resistance to BM212 mostly cluster in a specific region when mapped onto a structural model of MmpL3 (Fig. 6*C*), revealing a possible binding site. We conclude that BM212 inhibits TMM flipping across the IM by binding MmpL3 directly.

Discussion

How the mycobacterial OM is assembled is not well understood. Many members of the MmpL protein family are believed to be transporters that contribute to the assembly of various OM lipids (25–28); however, their specific roles have not been clearly defined. MmpL3 is the only member of this family essential for growth (5–7). Using two independent assays that allow determination of TMM topology in the IM of mycobacterial spheroplasts, and using putative inhibitors as molecular probes to modulate protein function, we have provided strong biochemical evidence that establishes MmpL3 as the TMM flippase. Whether MmpL3 is the only protein mediating TMM flipping or whether it is also involved in TMM release from the IM is not clear (Fig. 1*A*). One can posit that a second, still unidentified, protein may be necessary for extracting TMM from the IM and handing it to a putative chaperone. This scenario would be comparable to the transport of lipoproteins across the cell envelope in gram-negative bacteria (29). Alternatively, this step may also be mediated by MmpL3, in which case, flipping and release of TMM might be coupled, suggesting MmpL3 could interact with the putative chaperone. Extending from this idea, a third scenario may be possible where TMM flipping and release are essentially one single step in a mechanism similar to RND efflux pumps, whereby TMM never really resides in the outer leaflet of the IM. This latter model is, however, less likely because we have been able to decouple these steps by observing TMM translocation across the IM in our spheroplasts, which are effectively devoid of any putative chaperones. Moreover, despite being in the same RND protein superfamily, the structure of MmpL3 differs substantially from canonical RND efflux pumps (30). MmpL3 does form trimers like RND pumps (31), but the periplasmic domains of MmpL3 are much smaller (30) and it contains a large C-terminal cytoplasmic domain. Therefore, MmpL3 may not export TMM via an efflux mechanism. Further characterization of this system would be necessary to tease apart these models.

TB is one of the leading causes of death by infectious disease, and remains a major health problem worldwide (32). With the rapid emergence of multidrug-resistant and extensive drug-resistant TB, there is an urgent need to develop anti-TB drugs with novel mechanisms of action. In this regard, drugs inhibiting MmpL3, which has been shown to be an ideal target (33), would be especially important. Although many small molecules are thought to inhibit MmpL3, it is puzzling how molecules with

BIOCHEMISTRY

different molecular scaffolds may bind and target the same protein. We have now developed assays that measure the topology of TMM in the IM of mycobacterial spheroplasts, allowing the validation of true MmpL3 inhibitors. As a start, we have established that BM212 binds MmpL3 directly and inhibits its function. Furthermore, we have shown that SQ109, a molecule that has reached phase IIb clinical trials (Sequella), does not actually inhibit TMM flipping. In fact, it is likely that many of these molecules do not inhibit MmpL3 and have other targets, as has been shown for tetrahydropyrazo[1,5-*a*]pyrimidine-3-carboxamides (34). Our assays will help to select and advance small molecules currently under development as MmpL3-targeting drugs.

Materials and Methods

Detailed descriptions of all experimental procedures can be found in *SI Appendix*.

Assessing TMM Accessibility to Degradation by Purified LysB in Spheroplasts. *M. smegmatis* spheroplasts were metabolically labeled with sodium [1-^{14}C]-acetate for 2 h, followed by addition of purified LysB for 30 min at 37 °C. Lipids were extracted directly after the LysB treatment, analyzed by TLC, and visualized via phosphor imaging. Where indicated, putative MmpL3 inhibitors were added 15 min before addition of [^{14}C]-acetate.

6-Azido-TMM Surface Display Assay. *M. smegmatis* spheroplasts were metabolically labeled with 6-azido-trehalose for 2 h at 37 °C to synthesize 6-azido-TMMs, which were then reacted with Click-IT Biotin DIBO alkyne to generate biotin-TMMs. Surface-exposed biotin-TMMs were detected on spheroplasts using Alexa Fluor 488-conjugated streptavidin and visualized by fluorescence microscopy. Where indicated, putative MmpL3 inhibitors were added 15 min before addition of 6-azido-trehalose and included in all wash buffers.

BM212-MmpL3 Binding Assay. Purified MmpL3 was incubated with indicated concentrations of [^{14}C]-BM212 and/or cold BM212 for 30 min at room temperature. Samples were analyzed using Clear Native-PAGE, followed by phosphor imaging and Coomassie blue staining.

ACKNOWLEDGMENTS. We thank Graham Hatfull (University of Pittsburgh) for providing the pLAM3 plasmid for LysB overexpression, and Derek Lin (National University of Singapore) for constructing the inactive LysB$_{S82A}$ variant. We are grateful to Benjamin Swarts (Central Michigan University) for his generous gift of 6-azido-trehalose. We also thank Eric Rubin (Harvard School of Public Health) for providing strains, and for critical discussion and comments on the manuscript. We acknowledge Jasmine Chen (Mechanobiology Institute) for help with microscopy. This work was supported by National University of Singapore start-up funding, and by Singapore Ministry of Education Academic Research Fund Tier 1 and Tier 2 (MOE2014-T2-1-042) grants (to S.-S.C.).

1. Brennan PJ, Nikaido H (1995) The envelope of mycobacteria. *Annu Rev Biochem* 64:29–63.
2. Takayama K, Wang C, Besra GS (2005) Pathway to synthesis and processing of mycolic acids in *Mycobacterium tuberculosis*. *Clin Microbiol Rev* 18:81–101.
3. Banerjee A, et al. (1994) *inhA*, a gene encoding a target for isoniazid and ethionamide in *Mycobacterium tuberculosis*. *Science* 263:227–230.
4. Jackson M, et al. (1999) Inactivation of the antigen 85C gene profoundly affects the mycolate content and alters the permeability of the *Mycobacterium tuberculosis* cell envelope. *Mol Microbiol* 31:1573–1587.
5. Grzegorzewicz AE, et al. (2012) Inhibition of mycolic acid transport across the *Mycobacterium tuberculosis* plasma membrane. *Nat Chem Biol* 8:334–341.
6. Varela C, et al. (2012) MmpL genes are associated with mycolic acid metabolism in mycobacteria and corynebacteria. *Chem Biol* 19:498–506.
7. Domenech P, Reed MB, Barry CE, 3rd (2005) Contribution of the *Mycobacterium tuberculosis* MmpL protein family to virulence and drug resistance. *Infect Immun* 73:3492–3501.
8. Tahlan K, et al. (2012) SQ109 targets MmpL3, a membrane transporter of trehalose monomycolate involved in mycolic acid donation to the cell wall core of *Mycobacterium tuberculosis*. *Antimicrob Agents Chemother* 56:1797–1809.
9. La Rosa V, et al. (2012) MmpL3 is the cellular target of the antitubercular pyrrole derivative BM212. *Antimicrob Agents Chemother* 56:324–331.
10. Poce G, et al. (2013) Improved BM212 MmpL3 inhibitor analogue shows efficacy in acute murine model of tuberculosis infection. *PLoS One* 8:e56980.
11. Stanley SA, et al. (2012) Identification of novel inhibitors of *M. tuberculosis* growth using whole cell based high-throughput screening. *ACS Chem Biol* 7:1377–1384.
12. Remuiñán MJ, et al. (2013) Tetrahydropyrazolo[1,5-a]pyrimidine-3-carboxamide and N-benzyl-6′,7′-dihydrospiro[piperidine-4,4′-thieno[3,2-c]pyran] analogues with bactericidal efficacy against *Mycobacterium tuberculosis* targeting MmpL3. *PLoS One* 8:e60933.
13. Rao SP, et al. (2013) Indolcarboxamide is a preclinical candidate for treating multidrug-resistant tuberculosis. *Sci Transl Med* 5:214ra168.
14. Lun S, et al. (2013) Indoleamides are active against drug-resistant *Mycobacterium tuberculosis*. *Nat Commun* 4:2907.
15. Dupont C, et al. (2016) A new piperidinol derivative targeting mycolic acid transport in *Mycobacterium abscessus*. *Mol Microbiol* 101:515–529.
16. Dhiman RK, et al. (2011) Lipoarabinomannan localization and abundance during growth of *Mycobacterium smegmatis*. *J Bacteriol* 193:5802–5809.
17. Udou T, Ogawa M, Mizuguchi Y (1982) Spheroplast formation of *Mycobacterium smegmatis* and morphological aspects of their reversion to the bacillary form. *J Bacteriol* 151:1035–1039.
18. Udou T, Ogawa M, Mizuguchi Y (1983) An improved method for the preparation of mycobacterial spheroplasts and the mechanism involved in the reversion to bacillary form: Electron microscopic and physiological study. *Can J Microbiol* 29:60–68.
19. Bansal-Mutalik R, Nikaido H (2014) Mycobacterial outer membrane is a lipid bilayer and the inner membrane is unusually rich in diacyl phosphatidylinositol dimannosides. *Proc Natl Acad Sci USA* 111:4958–4963.
20. Payne KM, Hatfull GF (2012) Mycobacteriophage endolysins: Diverse and modular enzymes with multiple catalytic activities. *PLoS One* 7:e34052.
21. Gil F, et al. (2010) Mycobacteriophage Ms6 LysB specifically targets the outer membrane of *Mycobacterium smegmatis*. *Microbiology* 156:1497–1504.
22. Swarts BM, et al. (2012) Probing the mycobacterial trehalome with bioorthogonal chemistry. *J Am Chem Soc* 134:16123–16126.
23. Jewett JC, Sletten EM, Bertozzi CR (2010) Rapid Cu-free click chemistry with readily synthesized biarylazacyclooctynones. *J Am Chem Soc* 132:3688–3690.
24. Li W, et al. (2014) Novel insights into the mechanism of inhibition of MmpL3, a target of multiple pharmacophores in *Mycobacterium tuberculosis*. *Antimicrob Agents Chemother* 58:6413–6423.
25. Converse SE, et al. (2003) MmpL8 is required for sulfolipid-1 biosynthesis and *Mycobacterium tuberculosis* virulence. *Proc Natl Acad Sci USA* 100:6121–6126.
26. Jain M, Cox JS (2005) Interaction between polyketide synthase and transporter suggests coupled synthesis and export of virulence lipid in *M. tuberculosis*. *PLoS Pathog* 1:e2.
27. Pacheco SA, Hsu FF, Powers KM, Purdy GE (2013) MmpL11 protein transports mycolic acid-containing lipids to the mycobacterial cell wall and contributes to biofilm formation in *Mycobacterium smegmatis*. *J Biol Chem* 288:24213–24222.
28. Belardinelli JM, et al. (2014) Biosynthesis and translocation of unsulfated acyltrehaloses in *Mycobacterium tuberculosis*. *J Biol Chem* 289:27952–27965.
29. Okuda S, Tokuda H (2011) Lipoprotein sorting in bacteria. *Annu Rev Microbiol* 65:239–259.
30. Chim N, et al. (2015) The structure and interactions of periplasmic domains of crucial MmpL membrane proteins from *Mycobacterium tuberculosis*. *Chem Biol* 22:1098–1107.
31. Belardinelli JM, et al. (2016) Structure-function profile of MmpL3, the essential mycolic acid transporter from *Mycobacterium tuberculosis*. *ACS Infect Dis* 2:702–713.
32. WHO (2016) Global Tuberculosis Report 2016. Global actions and investments fall far short of those needed to end the global TB epidemic (WHO, Geneva), WHO/HTM/TB/2016.13. Available at www.who.int/tb/publications/global_report/en/. Accessed December 31, 2016.
33. Li W, et al. (2016) Therapeutic potential of the *Mycobacterium tuberculosis* mycolic acid transporter, MmpL3. *Antimicrob Agents Chemother* 60:5198–5207.
34. Cox JA, et al. (2016) THPP target assignment reveals EchA6 as an essential fatty acid shuttle in mycobacteria. *Nat Microbiol* 1:15006.
35. Kelley LA, Mezulis S, Yates CM, Wass MN, Sternberg MJE (2015) The Phyre2 web portal for protein modeling, prediction and analysis. *Nat Protoc* 10:845–858.